(Preprint) AAS 15-389

QUANTIFYING MAPPING ORBIT PERFORMANCE IN THE VICINITY OF PRIMITIVE BODIES

Thomas A. Pavlak,* Stephen B. Broschart,* and Gregory Lantoine,*

Predicting and quantifying the capability of mapping orbits in the vicinity of primitive bodies is challenging given the complex orbit geometries that exist and the irregular shape of the bodies themselves. This paper employs various quantitative metrics to characterize the performance and relative effectiveness of various types of mapping orbits including terminator, quasi-terminator, hovering, ping-pong, and conic-like trajectories. Metrics of interest include surface area coverage, lighting conditions, and the variety of viewing angles achieved. The metrics discussed in this investigation are intended to enable mission designers and project stakeholders to better characterize candidate mapping orbits during preliminary mission formulation activities.

INTRODUCTION

The exploration of small primitive bodies, such as comets and asteroids, is an area of active interest in the scientific community. Primitive body missions such as Dawn, Rosetta, and Hyabusa-2 are currently operating and a number of other missions, including OSIRIS-Rex, have planned launches in the next several years. While the specific scientific objectives of the various primitive body missions may vary, virtually all of them will include a surface mapping campaign to make scientific observations and improve knowledge of the primitive body shape model before beginning close-proximity operations. However, given the irregular shape of many primitive bodies of interest and the often non-Keplerian nature of orbits in their vicinity, predicting and assessing the quality of mapping observations can be difficult. This paper presents some quantitative characterizations to use as basis of comparison between different types of mapping orbits. This investigation leverages software developed at the Jet Propulsion Laboratory to design and assess the performance of various types of mapping orbits in the vicinity of primitive bodies including terminator,[1] quasi-terminator,[2] hovering,[3] ping-pong, and conic-like trajectories. The relative quality of mapping orbits is comparing using a number of metrics such as surface lighting conditions, spacecraft range and angles, and the variety in viewing geometry achieved.

PROBLEM DEFINITION

The goal of this investigation is to understand the trade space associated with carrying out remote sensing campaigns at small primitive bodies in the context of a robotic space mission. Specifically, this study seeks to understand the surface viewing geometries, ranges, etc. that are available from several commonly proposed mapping orbits architectures.

*Mission Design Engineer, Mission Design and Navigation Section, Jet Propulsion Laboratory, California Institute of Technology, 4800 Oak Grove Dr., Pasadena, CA 91109.

Remote sensing geometry

Remote sensing is the primary means of deriving science from an orbiting spacecraft. For the case of primitive body missions, examples of science investigations that rely on remote sensing include global map creation (in visible, infrared, etc.), shape modeling, and spectroscopy.

Generally, each type of remote sensing investigation has different optimal relative geometries between the spacecraft and the primitive body surface. These geometries can be described by four parameters: range, azimuth, incidence angle, and emission angle (Figure 1, Equations (1)-(4)).

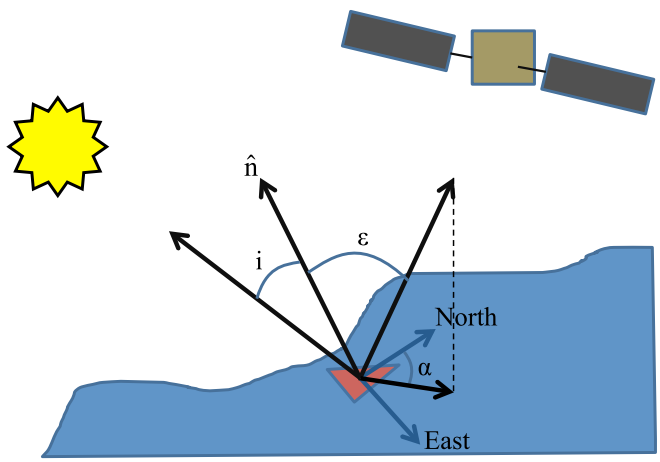

Figure 1. Mapping angles

$$r = ||\tilde{\mathbf{r}}_{sc,surf}|| \in [0, \infty) \text{ km} \tag{1}$$

$$\alpha = azimuth \in [0, 360) \text{ deg} \tag{2}$$

$$i = acos\left(\hat{n}^T\left(\tilde{\mathbf{r}}_{Sun} - \tilde{\mathbf{r}}_{surf}\right)\right) \in [0, 90] \text{ deg} \tag{3}$$

$$\epsilon = acos\left(\hat{\mathbf{n}}^T\left(\tilde{\mathbf{r}}_{sc} - \tilde{\mathbf{r}}_{surf}\right)\right) \in [0, 90] \text{ deg} \tag{4}$$

where $\tilde{\mathbf{r}}_{sc}$ is the spacecraft position relative to the center of the primitive body, $\tilde{\mathbf{r}}_{Sun}$ is the spacecraft position relative to the center of the primitive body, $\tilde{\mathbf{r}}_{surf}$ is the observed location on the primitive body surface, and $\hat{n}$ is the surface normal at the observed location. Often, the Sun-primitive body-spacecraft angle, known as the phase angle ϕ, is used as a proxy for incidence and emission. This is because the following constraint is (roughly) implied by the phase angle,

$$|i - \epsilon| \leq \phi \leq i + \epsilon \tag{5}$$

which implies,

$$\epsilon \geq \phi - i \tag{6}$$

and

$$\epsilon \geq i - \phi, \text{ if } (i - \epsilon) \geq 0, \tag{7}$$

or

$$\epsilon \leq i + \phi, \text{ if } (i - \epsilon) < 0, \tag{8}$$

Orbit possibilities near Primitive Bodies

The orbital dynamics near primitive bodies typically vary significantly from the nearly-Keplerian behavior that applies near planet-sized bodies. First, the mass distribution of these bodies differs significantly from spherically-symmetric. This introduces a strong perturbation to the orbit dynamics, which is usually poorly defined due to a lack of detailed knowledge of the internal mass distribution. Secondly, the magnitude of the gravitational attraction induced by these bodies is small enough so that other forces, including solar radiation pressure, comet outgassing acceleration, or gravity from other bodies, can become large relative to gravity. These forces can significantly change the character of the dynamics.

In the case of highly-perturbed dynamics, most orbits are destabilized and will ultimately escape or crash into the body surface. There are only a select number of orbits that have been described to date which are stable over long periods of time in these environments. A selection of both stable and unstable orbits that are relevant to current and future primitive body mapping applications are examined in this investigation.

Mission Operations Considerations

The problems associated with selecting orbits for remote sensing campaigns are addressed here assuming the context of a robotic space mission operated entirely by a team on Earth (i.e., without any significant and relevant on-board capabilities). Some particular constraints are implied by this, mostly related to time. Generally, it can be assumed that maneuvers should not be planned more often than about once a day. The reason for this is that the summation of the time needed to accumulate measurements after a maneuver, round-trip light time, time for orbit determination and maneuver design, testing, sending the commands to the spacecraft, and any unexpected time delays during that process induce significant risk if less time is allowed. Further, operations at that frequency are very intense for a ground team and this limits the amount of time they can be maintained without introducing significant risk associated with human factors. Generally, a sustainable remote sensing campaign should not require maneuvers or other on-board updates more often than about twice a week.

There is also usually a desire to keep the fuel used by the spacecraft to a minimum as such mass is usually at a premium. For primitive body missions, however, this constraint is usually less restrictive since the amount of fuel needed to manipulate the slow spacecraft speeds around the primitive body usually represents a very small fraction of the spacecraft mass.

Finally, there is a priority placed on stable spacecraft orbits, or at least orbits that do not risk impact if the spacecraft is unattended for weeks at a time. The typical response to a significant on-board anomaly is to put the spacecraft into a “safe-mode”, where the ability to perform maneuvers would generally be disabled. Since a safe-mode can occur any time, it is desirable to avoid being on a trajectory that will risk the spacecraft in any way within a few weeks.

PREVIOUS WORK

Several orbit strategies have been developed with the implicit goal of supporting remote sensing campaigns at small primitive bodies. Each approach has strengths and weaknesses, several of which will be quantified in the following sections. Figure 2 shows examples of the various trajectory strategies to be discussed in this section.

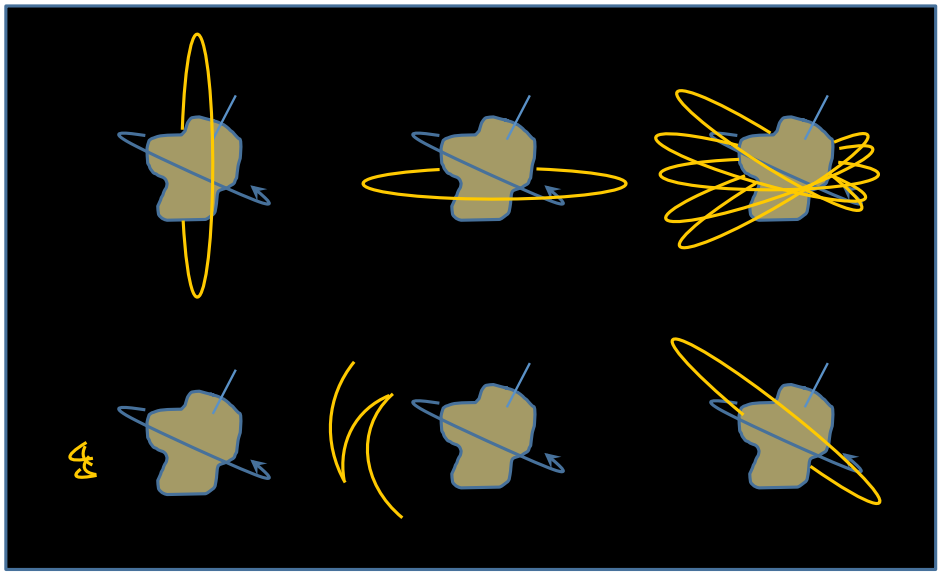

Figure 2. Various trajectory strategies for global remote sensing at primitive bodies. In all cases, the Sun is to the left of the figure. (top row, left to right) Terminator orbits, ecliptic orbits, and quasi-terminators; (bottom row) hovering, ping-pong, and orbit maintenance strategies.

Orbital observation strategies

Terminator orbits[4,5,6,7] are appropriate for dynamics where the orbit perturbation from solar radiation pressure (SRP) is significantly stronger than that from the irregular gravity distribution of the body. These orbits balance the SRP acceleration against the pointmass gravity of the body by maintaining an orientation where the orbit normal points either directly toward or away from the Sun. The orbits are roughly conic in shape and the nominal eccentricity is chosen such that the nodal precession rate matches the mean motion of the central body around the Sun. Terminator orbits are known to be very stable,[8] which is a useful property for primitive body missions where the details of the central body mass distribution are not known *a priori*. The primary drawback of terminator orbits is that the phase angle ϕ of the spacecraft is always 90 deg or more, which limits the possible viewing geometries of the surface. NASA's OSIRIS-REx mission plans to use terminator orbits for precision gravity and shape modeling.[9]

In strong SRP dynamical environments, another class of potentially stable orbits exist in the ecliptic plane of the body.[5,6,7,10] Ecliptic orbits can offer improved visibility of the band on the body near the ecliptic. However, these orbits become increasingly eccentric as SRP increases until periapsis lies below the surface of the primitive body. In such cases, there are variations of ecliptic orbits that use orbit maintenance maneuvers to maintain a non-impacting trajectory. These non-ballistic orbit options, including alternating orbits,[11] heliotropic orbits,[12,13,14] or simply maintained conic orbits, can offer surface viewing geometry similar to stable ecliptic orbits. While ecliptic orbits often require orbit maintenance, the maneuver frequency may be acceptable.[15]

Quasi-terminator orbits[16] are a variation on the terminator orbits where the spacecraft is able to make significant departures from the terminator plane, while retaining the stability associated with terminator orbits. The deviation from the terminator plane can greatly improve the viewing geometry compared to terminators by pushing the minimum phase angle down to 45 deg or less.

However, quasi-terminators are not applicable for all situations as they require a particular balance of solar radiation pressure strength, primitive body mass, and heliocentric range for most applications. Generally, this range is consistent with the environment around small near-Earth objects, but not main-belt asteroids or comets. Quasi-terminators have been considered for use in an extended orbit phase for JAXA's Hayabusa2 mission.[17]

Actively manipulated trajectory strategies

Hovering[18,19] is a spacecraft control strategy where the thrusters are used to maintain the spacecraft location at a (nearly) fixed point. The location can be fixed in either the body frame or relative to the Sun. Hovering is possible for smaller primitive bodies because the gravitational acceleration is small enough to keep the delta-V costs reasonable. Hovering can achieve arbitrary viewing geometries when a sequence of hovering positions are linked together. However, fuel is needed to maintain the hovering position, which can become significant over time. Also, if the hovering control system were to fail, the time to impact may be short. Hovering was implemented as the station-keeping strategy during the global mapping campaign of JAXA's Hayabusa mission[20,21] and is planned for use on Hayabusa2 as well.[22]

A ping-pong "orbit" is actually a sequence of orbit segments joined by maneuvers. Often, the segments are hyperbolic with the notion that, if the spacecraft were to fail to execute a maneuver, it would safely escape from the body. When done at reasonable range from the body, ping-pong orbits are insensitive to uncertainty in the dynamical environment and can achieve any desired relative viewing geometry. The downside of ping-pong orbits is that the maneuver frequency can be high and it is difficult to maintain them over long periods of time due to fuel cost (and maneuver frequency). A ping-pong approach was used by ESA's Rosetta mission to support characterization of comet Churyumov-Gerasimenko[23] and is planned for part of the characterization phase for NASA's OSIRIS-REx mission.[24]

Another active control option is to plan on regular orbit maintenance to support a slowly varying Keplerian orbit geometry. This can be a feasible approach if the non-Keplerian perturbation is not so strong as to require frequency orbit correction or large expenditures of fuel.[15] The advantage of this approach is that a full range of orbit nodes and inclinations could potentially be implemented, allowing for a remote sensing campaign that is very similar to that at a planetary body.

APPROACH

The dynamical environments near small primitive bodies are often complex. The relative influence of gravity, solar radiation pressure, and tidal forces are dependent on the size, shape, and solar distance of the body as well as the altitude of the spacecraft. Thus, the design of spacecraft trajectories in the vicinity of primitive bodies is nontrivial. In this investigation, mapping orbits are designed using JPLs Small Body Dynamics Toolkit (SBDT) that supplies shape and gravity models for a variety of primitive bodies. For this analysis, a polyhedral mesh consisting of thousands of triangular facets is employed to represent the primitive body shape. The gravitational environment is consistent with the Augmented Circular Restricted Three-Body Problem (ACR3BP) that models the Sun and primitive body as gravitational point masses, assumes the Sun and body orbit their common barycenter in circular co-planar orbits, and also includes the effects of solar radiation pressure (SRP).

Computing Primitive Body Coverage

Once a potential trajectory is computed, the metrics used to assess its mapping performance are computed via the Primitive Body Coverage and Geometry Evaluator (PB-CAGE) software tool – an add-on for SBDT that is implemented in Matlab. Given a spacecraft trajectory, pointing direction, and instrument properties, PB-CAGE computes the surface elements of the polyhedral shape model that are in view of the instrument at each user-specified observation epoch. The software package is also capable of computing self-shadowing – when part of the body blocks another part of the body from the Sun – and self-obstruction – when part of the body blocks the spacecraft's view of another part of the body – which are both important considerations in the case of irregularly-shaped primitive bodies. An example of a sequence of observations for an orbit in the vicinity of Itokawa is depicted in Figure 3. The shaded blue squares represent the polyhedral facets in view of the instrument at each observation epoch, the spacecraft appears as a magenta dot, and the spacecraft instrument boresight vector is illustrated in green. PB-CAGE computes a variety of coverage metrics

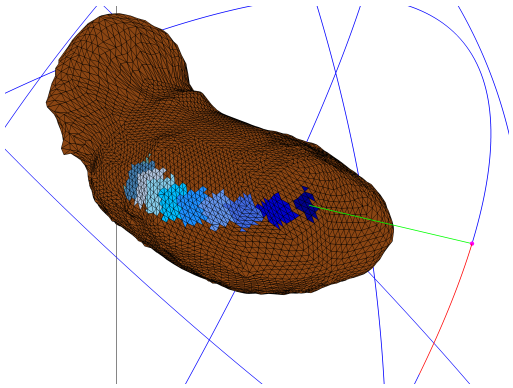

Figure 3. Example Observation Sequence along a Polyhedral Representation of Itokawa

at each observation time including spacecraft range, emission angle (the angle between the surface normal and body-spacecraft vectors), incidence angle (the angle between the surface normal and the body-Sun vectors), and spacecraft and solar azimuth angles. The results are then post-processed to produce any desired mapping orbit performance comparison metrics, e.g., incidence angle vs. emission angle, percentage of surface area coverage vs. time, etc.

Assumptions

The pointing of a particular instrument can introduce many complex constraints that limit the possibilities for remote sensing. In this study, we assume that the instrument field-of-view always covers all of the primitive body surface that is visible from the spacecraft. This eliminates the need to consider an instrument pointing profile. As such, the results here present the set of what is geometrically possible. Similarly, we assume that the instrument can observe the body at any time. Typically, scheduling of various spacecraft activities limits instrument observation times, but that is a spacecraft specific constraint.

In this investigation, several assumptions are also made concerning the primitive body, itself. First, it is assumed that the body is a spherical, faceted polyhedron. Unlike irregularly-shaped primitive bodies, the surface geometry of a sphere is longitude-independent, making it easier to generalize the results of this analysis. Under these assumptions, the surface of the primitive body

is not smooth, but, rather, consists of a discrete number of triangular facets. PB-CAGE does not compute partially observed facets; if greater than half the facet is visible, the entire facet is considered visible. Thus, the instrument's observational footprint on the surface consists of the discrete collection of visible facets. Lastly, to further generalize the results, it is assumed that orientation of the primitive body spin pole is fixed with respect to the Sun for the duration of each simulation. Four fixed pole orientations, depicted in Figure 4, are considered in this study. P1 is aligned with the body-Sun vector, P2 is aligned with ecliptic north, P3 is defined such that P3 = P2 $\times$ P1, and P4 is consistent with a 30 degree rotation of the P2 pole vector about P3.

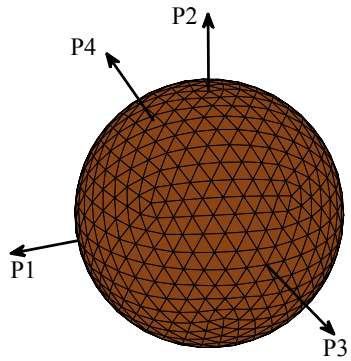

Figure 4. Pole orientations

RESULTS

In this preliminary analysis, the primitive body surface coverage possible from various orbit types is characterized with respect to incidence angle, emission angle, and, to a lesser extent, azimuth as a function of surface latitude for various pole orientations. Using a spherical polyhedral body, PB-CAGE is leveraged to compute surface observation data for a variety of representative mapping orbits. For each orbit and pole orientation – P1, P2, P3, or P4 – the available viewing geometries are characterized by plotting incidence angle vs. emission angle for each *lit* spacecraft observation. The plots are colored by latitude ranging from 0 to 90 degrees in increments of 10 degrees and, given the discrete nature of the polyhedral body's surface, latitude bins of width ± 5 degrees are utilized. For clarity, only the outer boundary of each colored region is shown.

Terminator Orbits

The family of stable terminator orbits typically spans a reasonable range of semi-major axes, bounded on the high side and the irregular body gravity on the low side. When SRP is strong (as in the case considered here), eccentricities of these orbits tend to be low, so the range is fairly consistent around the orbit. Even in cases of mild SRP where the periodic terminator solution has some eccentricity, a non-periodic terminator with zero eccentricity is usually stable. As such, the range to the surface for terminator orbits is usually consistent across the orbit with a set of possibilities dictated by the relative strength of SRP and the spin and irregularity of the target body's mass distribution.

Incidence and emission angle possibilities for terminators are relatively limited since the phase angle of these orbits is always greater than 90 deg (see Equation (6)). The range of possible in-

cidence and emission combinations for the P1, P2, and P4 pole orientations are shown in Figures 5(a), 5(c), and 5(e), respectively. For the particular orbit chosen for these plots, the phase angle is nearly constant at around 100 deg. The diagonal boundary in all three plots clearly demonstrates the phase angle constraints in Equations (6)-(8). For all three pole orientations, the constraint is given by Equation (6) alone, since the right-hand side of Equation (7) is always negative and the right-hand side of Equation (8) is always greater than 90 deg.

Terminator orbits are approximately axially symmetric around the Sun-line, so the pole orientations presented in Figures 5(a), 5(c), and 5(e) effectively cover all possibilities. In the P1 configuration (Figure 5(a)), the incidence angle and latitude on the body are tightly constrained such that $i = 90$ deg $- lat$, which results in the banded results shown. For the case of the P2 pole, the incidence angle at a particular latitude can be anywhere in the range from zero to 90 deg as the body rotates. For the skewed P4 pole, the range of incidences varies by $\pm(90$ deg $- lat)$ around the angle between the pole and the Sun direction.

The range of potential azimuth angles from terminator orbits covers nearly the full compass for the P2 pole orientation, except for gaps that emerge due to the offset of the orbit center in the anti-Sun direction. Locations near the sub-solar point cannot be seen at all because of the self obstruction due to this offset and the finite range from the body as illustrated with dashed lines in Figure 6(a). Also, at high incidence angles (i.e., near the terminator), due north or south azimuths (0 or 180 deg) are not possible when the incidence is less than 90 deg, i.e., when lit. For the P1 (subsolar-pointing) pole orientation, a spacecraft in a terminator orbit is only visible at southern azimuths.

Ecliptic Orbits

The range associated with orbits in the ecliptic plane is largely manageable as a design variable. As mentioned earlier, the truly periodic, near-conic ecliptic orbits have very large eccentricities for high-SRP cases. Since this high eccentricity results in sub-surface periapsis, this orbit type is not relevant. For this analysis, it is assumed that either: 1) the SRP is weak enough such that a reasonable eccentricity results, 2) a highly non-Keplerian approach, such as alternating orbits,[11] is used, or 3) orbit maintenance is used to maintain a conic orbit with desirable characteristics. In all cases that are consistent with ground navigation, the range will be bound similarly to the terminator case: the maximum is dictated by the SRP strength and the minimum by the mass distribution and spin state of the body.

The range of possible incidence and emission combinations for ecliptic orbits for the three pole orientations are shown in Figures 5(b), 5(d), and 5(f). For these orbits, a full range of phase angles is achieved by the spacecraft (from 0 to 180 deg), which generally results in good coverage of incidence-emission space for the low- to mid-latitudes. In the P1 case, the incidence angles and latitudes are again equal, which results in the banded pattern shown in Figure 5(b). However, within that constraint introduced by the pole orientation, incidence-emission angle coverage is complete since the rotation of the body and the complete range of phase angles allows for all emission angles to be seen from the spacecraft orbit. For the P2 orientation, coverage of low- to mid-latitudes is excellent, on account of both the incidence and phase angles independently covering the full range of possibilities. However, due to the pole geometry, coverage becomes worse at high latitudes, with some area around the pole not visible at all due to self-obstruction of the body. Though Equation (6) suggests a lower bound on emission, the orbit geometry relative to the pole limits the emission angle to a minimum of the latitude of the observed location. For the P3 pole orientation, all incidence angles are available above the surface location latitude, but the emission possibilities are limited.

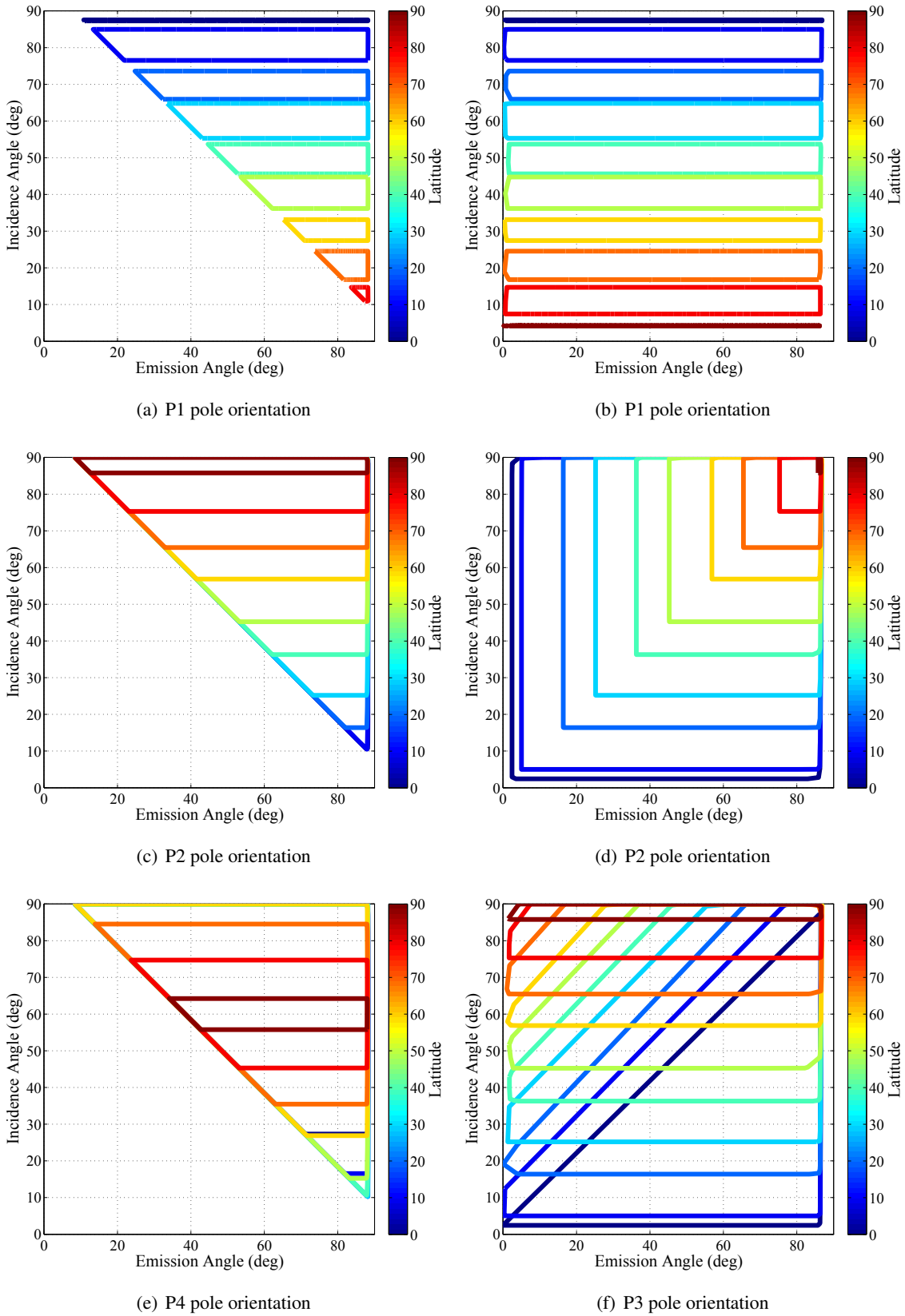

(a) P1 pole orientation

(b) P1 pole orientation

(c) P2 pole orientation

(d) P2 pole orientation

(e) P4 pole orientation

(f) P3 pole orientation

Figure 5. Inicidence and emission possibilities for terminator (a, c, e) and ecliptic (b, d, f) orbits

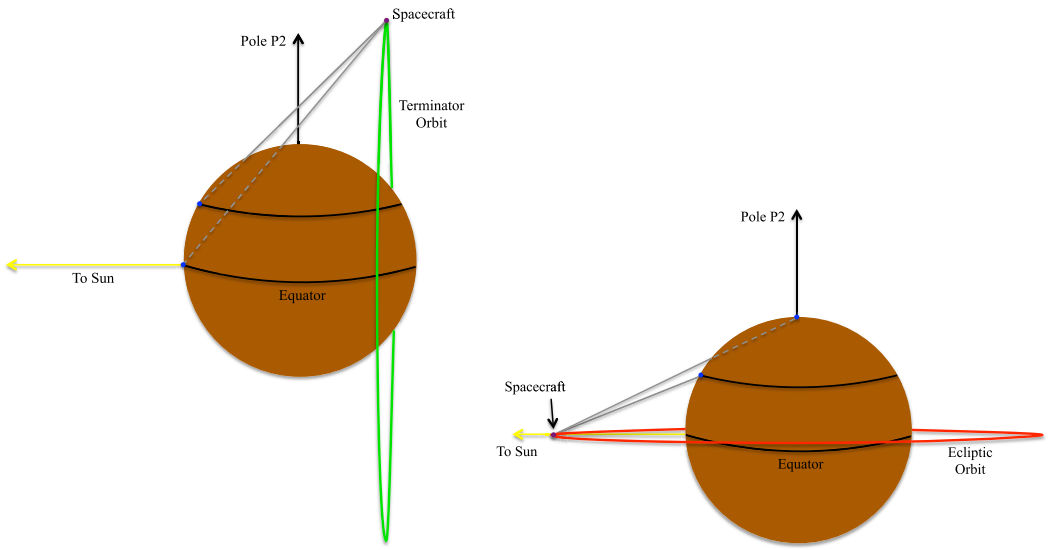

(a) Terminator orbit

(b) Ecliptic orbit

Figure 6. Achievable azimuths for terminator (top) and ecliptic (bottom) orbits with the P2 pole orientation

In this case, the 0 deg emission case is available at all latitudes, but only when they pass through the plane of the orbit. When the location rotates out of the plane, incidence decreases, but emission must as well. Note that, in reality, the colored regions in Figure 5(f) are triangular, but appear as polygons due to the ± 5 deg latitude bins used in this analysis.

The ecliptic orbits more-or-less yield a full spectrum of the possible azimuth angles. As mentioned before, there is a small region around the pole that may not ever be seen due to self-obstruction. Also, there are deficiencies introduced by the P2 pole orientation where the northern hemisphere is only seen from the south, and the southern hemisphere only from the north. True east and west azimuths are only possible at the equator, as depicted in the schematic in Figure 6(b).

Quasi-Terminator Orbits

In useful quasi-terminator orbits, the orbit eccentricity is always significant. For Sun-side quasi-terminators (where apoapsis is on the lit side of the body), there is significant variation between the apoapsis altitude, which is achieved at the minimum phase angle, and the altitude at the terminator. For the dark-side quasi-terminators, the variation on the lit side of the body is less dramatic and those altitudes are relatively low. There is a strong correlation between the minimum and maximum orbit altitudes for terminators and the minimum phase angle. The relationship between these quantities varies with the strength of the solar pressure. In all cases, the apoapsis altitude is significantly higher than an equivalent energy terminator orbit.

Quasi-terminators can have excellent coverage in the incidence-emission space, as shown in Figures 7(a), 7(c), and 7(e). In many ways, these results are similar to those of terminator orbits, with the key difference is that the lower-left boundary dictated by the minimum phase angle is much lower. It is important to note that the minimum altitude decreases as the phase angle decreases, so the relative SRP-strength must be in the appropriate range to achieve similar results. Also, like the

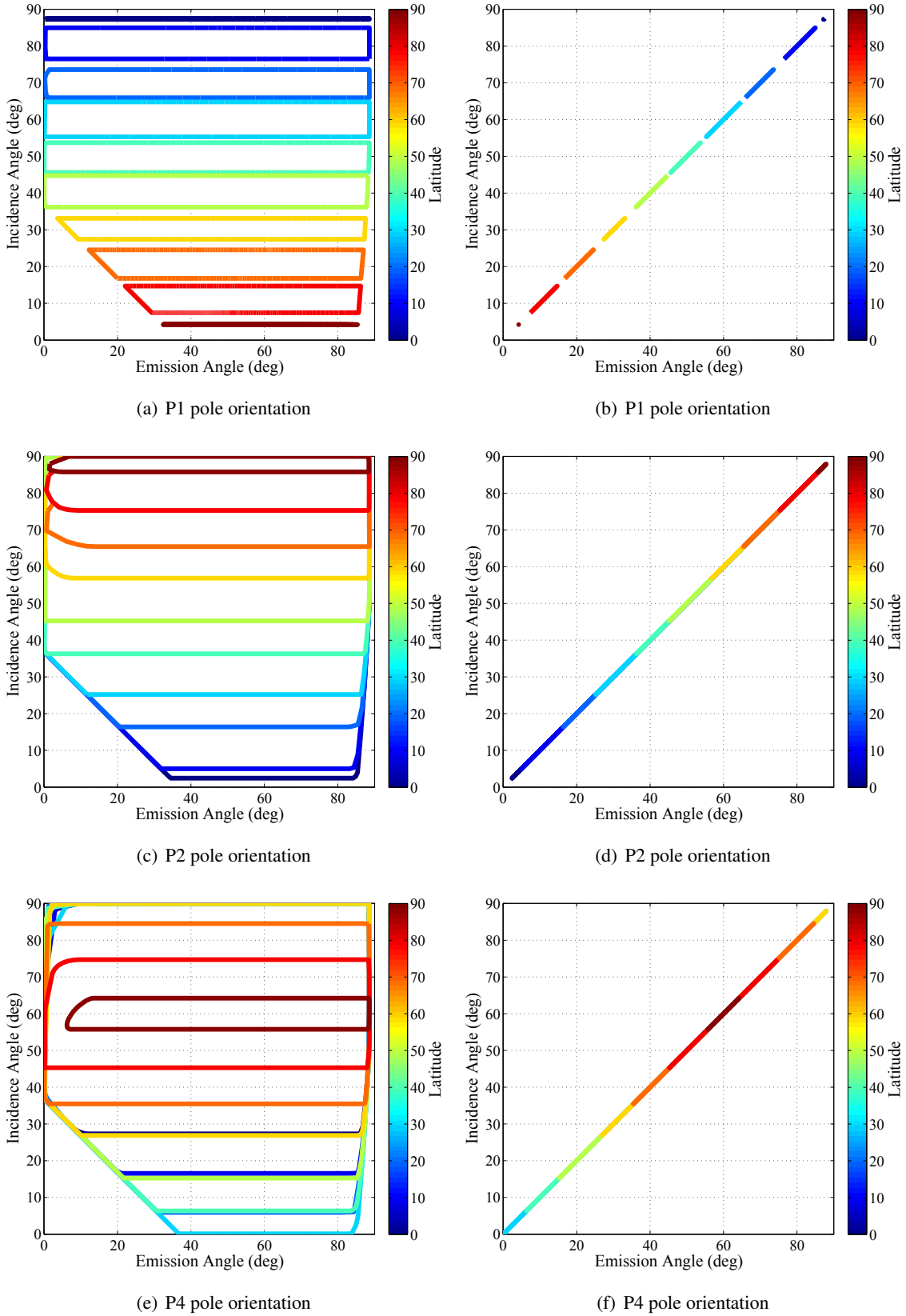

(a) P1 pole orientation

(b) P1 pole orientation

(c) P2 pole orientation

(d) P2 pole orientation

(e) P4 pole orientation

(f) P4 pole orientation

Figure 7. Inicidence and emission possibilities for quasi-terminator (a, c, e) and hover (b, d, f) orbits

terminators, these orbits are effectively axially symmetric so these three plots describe the entire set of possibilities.

Quasi-terminators also do very well with regard to azimuth since the orbit plane varies constantly. Over time, the quasi-terminator orbits can cover the full range of azimuth possible. Though the quasi-terminator orbits offer a very wide range of surface relative orientations, it is important to note that it takes longer to achieve this range because the orbit must move at its natural pace through the range of possibilities.

Hovering

Assuming the spacecraft has adequate maneuvering capability, there are an infinite variety of hovering trajectories available. Of course, the spacecraft range and fixed (or nearly fixed) location with respect to the body-fixed or sun-body synodic frames dictates the spacecraft's set of achievable observation geometries. In this analysis, a subsolar hovering trajectory is assumed.

Unlike the terminator and quasi-terminator trajectories, the incidence-emission space for the subsolar hovering orbit is linear as illustrated in Figures 7(b), 7(d), and 7(f). For the subsolar-pointing P1 pole orientation, each latitude on the body is observed at a single incidence-emission angle pair and the resulting incidence vs. emission plot consists of a series of points (though Figure 7(b) appears as lines due to the latitude binning discussed previously). As with the P1 case, the P2 and P4 cases also clearly exhibit the constraint, $\epsilon + i = 90$ deg. For the P2 pole, the poles are observed only at high incidence and emission angles, while the equatorial latitudes are seen at a wide range of angles $\epsilon, i \in [0, 90]$ deg. The effect of the pole tilt in the P4 case is evident in 7(f), most noticeably for the polar region of the body which is only visible at incidence and emission angles equal to the declination of the pole (60 deg).

Ping-Pong Orbits

Like the hovering trajectories, ping-pong orbits are governed largely by the spacecraft's maneuver capability (with respect to burn magnitude and frequency). However, unlike the hovering trajectories which loiter near a fixed location, ping-pong orbits are fundamentally arbitrary and can achieve virtually any surface observation geometry. While the particular achievable incidence-emission regions presented in Figures 8(a)-8(c) are arbitrary, the figures are intended to be representative and to demonstrate that an appropriately-designed ping-pong trajectory can yield an abundance of potential surface observing geometries.

Orbit Maintenance

Incidence/emission results are not presented for the orbit maintenance approach in this investigation, however, this mapping strategy is generally capable of achieving results consistent with "typical" conic orbiters (ecliptic, equatorial, polar, etc.) at the cost of maneuver delta-V and frequency. Of course, the orbit must also be dynamically feasible given the SRP and often irregular gravity perturbations associated with a primitive body of interest.

CASE STUDY

The incidence vs. emission angle plots presented in the previous section provide a useful means of visually assessing the variety of surface observation geometries that are achievable by a given mapping orbit. However, it is also informative to have qualitative metrics for assessing the mapping

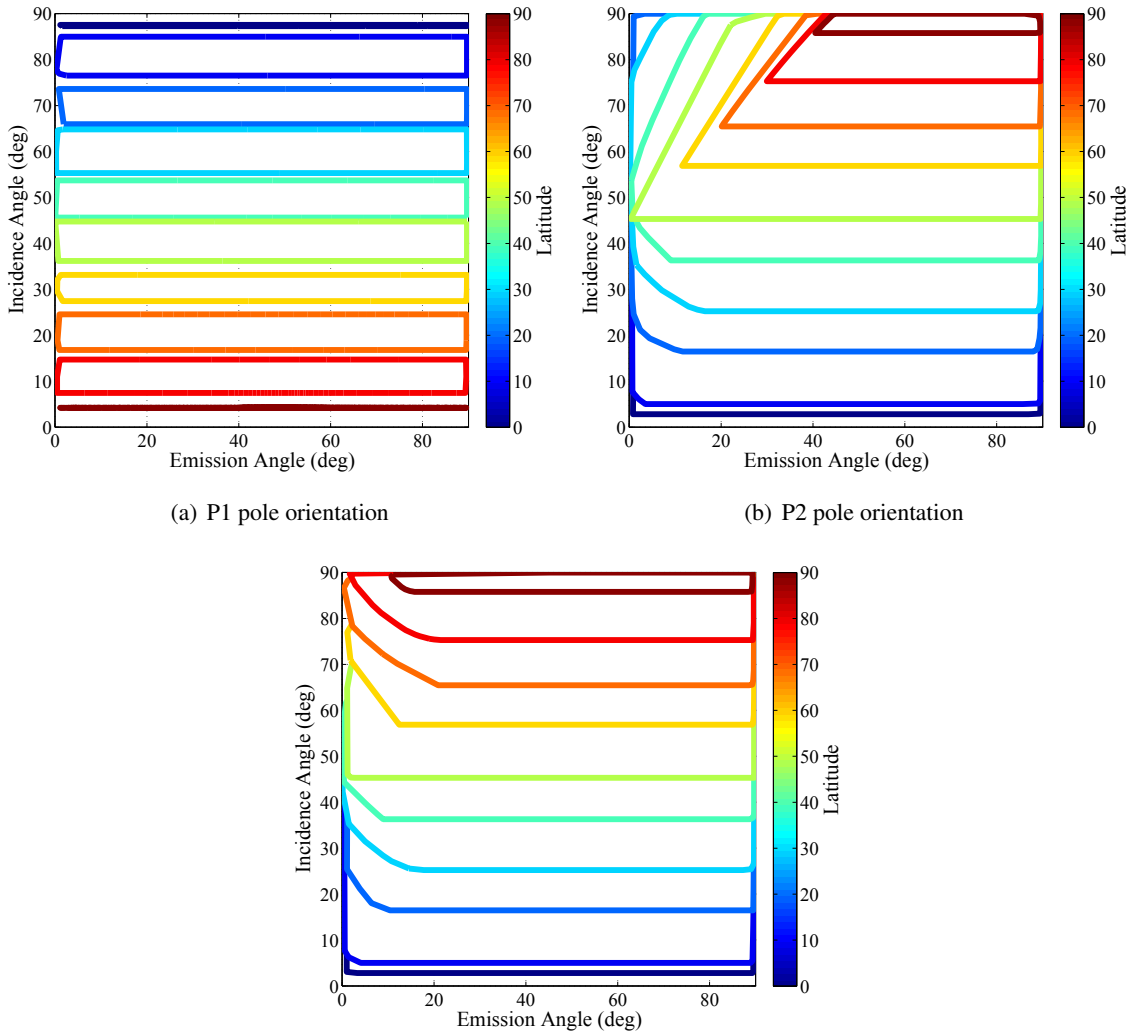

(a) P1 pole orientation

(b) P2 pole orientation

(c) P3 pole orientation

Figure 8. Incidence and emission possibilities for ping-pong orbits

performance of various candidate trajectories. Thus, this analysis employs a case study to demonstrate the application of nine useful metrics to a representative primitive body and set of example mapping orbits.

Test Primitive Body

To remove the effects of rotation rate and local surface geometry from the primitive body mapping assessment, a spherical body that is phase-locked with the Sun is assumed. For purposes of this analysis, a normalized β acceleration of 25 is also assumed, where

$$\beta = \frac{G_1}{\left(\frac{m}{A}\right) \mu_S^{2/3} \mu_{PB}^{1/3}} \tag{9}$$

and G_1, μ_S, μ_{PB}, m, and A denote the solar flux, solar gravitational parameter, primitive body gravitational parameter, spacecraft mass, spacecraft cross-sectional area, respectively. In this study, the relevant constants are defined as follows:

$$G_1 = 1 \times 10^{14} \frac{\text{kg} \cdot \text{km}}{\text{s}^2} \tag{10}$$

$$\mu_S = 1.327 \times 10^{11} \frac{\text{km}^3}{\text{s}^2} \tag{11}$$

$$m = 1100 \text{ kg} \tag{12}$$

$$A = 14 \text{ m}^2 \tag{13}$$

Given $\beta = 25$ and assuming a uniform density of the primitive body of 1 g/cm^3, the mass parameter and radius of the spherical primitive body are computed. Using the assumed β and density, the spherical primitive body has a gravitational parameter, μ_{PB}, and radius, r, of 1.3415×10^{-8} km^3/s^2 and 363 m, respectively. A polyhedral representation of the primitive body with 1,280 facets is used throughout this case study.

EXAMPLE TRAJECTORIES

Five representative primitive body mapping orbits are leveraged to assess the effectiveness of various mapping metrics described in this study:

1. Quasi-terminator orbit (blue)
2. Terminator orbit (green)
3. Ping-pong orbit (black)
4. Ecliptic orbit (red)
5. Hover orbit (magenta dot)

The example trajectories are depicted in a Sun-primitive body synodic coordinate frame in Figure 9; the trajectory colors are defined in the list above.

MAPPING METRICS

This investigation utilizes a variety of quantitative metrics and combinations of metrics to characterize the mapping performance of a given trajectory and to compare the relative effectiveness of multiple candidate mapping orbits. While some mapping metrics may be mission/instrument specific, other metrics are relevant to many primitive body missions. For example, virtually all missions will be concerned with the percentage of surface coverage and variety of viewing geometries achieved. It is useful to consider the percentage of coverage as a function of time and also the number of times each facet of the polyhedral shape model is observed. To ensure that surface observations are made at a variety of spacecraft and solar geometries, considering observations in the incidence angle-emission angle space provides valuable insight. For mapping surface landmarks, surface pixel resolution and minimum/maximum spacecraft range is likely a useful metrics. These metrics and others presented in this investigation are intended to offer a mission designers and stakeholders a means of quantitatively comparing the effectiveness of various candidate mapping orbits.

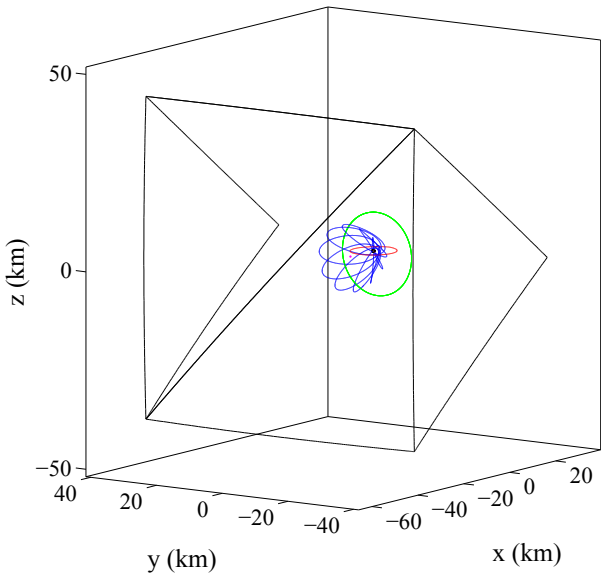

Figure 9. Example trajectories used for case study

To condense the large quantity of PB-CAGE output data into concise mapping metrics, five key pieces of data are required: orbital period, surface area coverage, spacecraft range, emission angle, incidence angle, and frequency of required maneuvers. The orbital period and frequency of required maneuvers are properties of the mapping orbits, themselves, and are, effectively, user-provided inputs. The other four items are computed by PB-CAGE in accordance with a user-specified observation cadence.

The surface area coverage is reported as a percentage and is computed by summing the surface areas of polyhedral facets observed by the spacecraft up to and including the current observation time. Spacecraft range is simply the distance from the spacecraft to the center of the primitive body. Emission, incidence, and phase angles have been defined previously. It is important to note that, in this case study, only *lit* observations of the primitive body are considered.

Leveraging PB-CAGE raw output, it is possible to generate a variety of useful three-dimensional figures depicting various mapping metrics over the surface of the primitive body, however, inferences drawn from these figures are often only qualitative. Thus, this analysis also proposes the use of the following nine quantitative metrics to characterize the relative mapping effectiveness of candidate trajectories:

1. Orbital period
2. Percentage of surface area coverage achieved in one period
3. Mean spacecraft range
4. Minimum phase angle
5. Range at minimum phase angle
6. Mean phase angle

7. Standard deviation of phase angle

8. Standard deviation of mean emission angle

9. Frequency of required maneuvers

Orbital Period

For the quasi-terminator, terminator, and ecliptic orbits, the orbital period is simply the time required for the spacecraft to return to its starting position in the synodic reference frame. Total time of flight is used in place of orbital period for the non-periodic ping-pong and hover orbits. Orbital period is an easily-computed metric that provides some insight into the frequency at which spacecraft-primitive body observation geometries will repeat and the total duration required to complete the mission's mapping objectives.

Percentage of Surface Area Coverage Achieved in One Period

Combined with orbital period, the percentage of surface area coverage achieved in one period expresses how much of the body is observed in a single orbit and the duration required to achieve that coverage. Generally, shorter duration mapping campaigns are preferable for a variety of operational and programmatic reasons so the percentage of surface area coverage achieved in one period is useful information during preliminary mission design activities.

Mean Spacecraft Range

Mean spacecraft range simply provides a metric for how close, on average, a candidate mapping orbit is from the primitive body. Spacecraft range is potentially important depending on the spacecraft instrumentation and the scientific and navigation requirements.

Minimum Phase Angle

The minimum phase angle essential represents how close the spacecraft passes to the sub-solar point on the primitive body. This is important because the sub-solar point is the best lit, warmest, and, in the presence of outgassing phenomena, potentially the most volatile region of the body.

Range at Minimum Phase Angle

This metric is simply the spacecraft distance to the center of mass of the primitive body at minimum phase angle. From a instrument resolution standpoint, lower ranges at minimum solar phase angle are preferable.

Mean and Standard Deviation of Phase Angle

Taken together, the mean and standard deviation of the solar phase angle, ϕ, provide a picture of the typical phase angle provided by a candidate mapping orbit as well as the range of phase angles achieved. A moderate mean phase angle combined with a high standard deviation, for example, implies that the mapping orbit achieves a variety of geometries relative to the sun – a desirable mapping orbit characteristic.

Standard Deviation of Mean Emission Angle

For a phase-locked primitive body, the incidence angle for each polyhedral facet is constant (since its orientation relative to the Sun does not change). Thus, it is particularly useful, in this case, to assess the effectiveness of a mapping orbit via the standard deviation of the mean *emission angle*. The mean emission angle is illustrated for each of the five example trajectories in Figure 10. Fundamentally, a *large* standard deviation in phase angle is desirable because it means that the orbit offers a variety of surface observation geometries. It is desirable that the Std(ϕ) is large and standard deviation of the mean emission angle is *small*, implying that 1) the facets are visible with a variety of geometries and 2) that all facets have a similar mean emission angle and, thus, all observed with geometries that are equally variety.

MAPPING METRICS FOR EXAMPLE TRAJECTORIES

To assess the effectiveness of the nine mapping metrics described in the previous section, the metrics are applied to analyze the five candidate mapping orbits outlined in Section and the results are depicted in Table 1.

Table 1. Mapping metrics for example trajectories

	Period (days)	% Coverage (1 period)	Mean Range (km)	Min. Φ (deg)	Range at Min. Φ (km)	Mean Φ (deg)	std Φ (deg)	std mean emission (deg)	Mnvr Freq.
QTO	113.02	50.91	10.94	36.77	13.62	49.85	20.91	4.14	N/A
Terminator	21.91	50.09	10.7	98.38	10.54	98.42	0.0296	11.27	N/A
Ping Pong	73.33	50.91	56.95	6.33	43.57	53.62	21.96	4.59	x 10 days
Equatorial	9	50.91	5.91	7.7	6	90.81	53.56	11.06	x 5 days
Hover	45	48.5	10	0	10.04	0	0	21.23	Cont.

For each of the five example orbits, the nine mapping metrics yield quantitative results that, when analyzed in concert, provide valuable insight into the relative effectiveness of the mapping trajectory in question. Each of the five orbits are able to observe approximately 50% of the body when lit – an expected result given the phase-locked nature of the primitive body.

The terminator and hover orbits maintain constant distances from the body that are approximately equal. The QTO observes the body at a similar mean range despite the fact that its ranges varies significantly during the course of an orbit.

The minimum phase angles achieved by the ping-pong, ecliptic, and hover orbits are all relatively low (less than 8 degrees) given that they pass near the sub-solar point on the primitive body. The minimum phase angle of the QTO is consistent with the user-defined design parameters of the trajectory. The terminator orbit, which is nearly polar, has a minimum phase angle near 90 degrees as expected.

The two most telling parameters in this analysis are, perhaps, standard deviation of the phase angle and standard deviation of the mean emission angle. The equatorial orbit has the largest standard deviation of ϕ meaning that it observes the greatest variety of phase angles, however it also has a larger standard deviation of the mean emission angle because there is little variation in the geometry when it is observing the poles of the body. As one would expect, the terminator orbit exhibits little variation in observation geometry, possessing a vary small standard deviation of ϕ (because it only

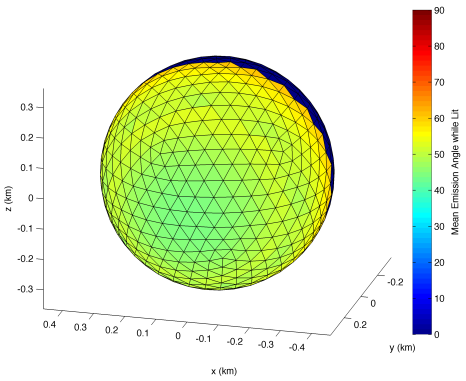

(a) Quasi-Terminator Orbit

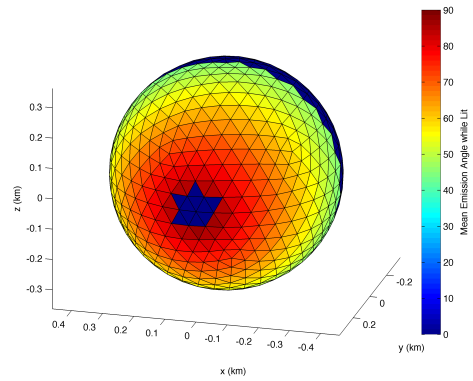

(b) Terminator Orbit

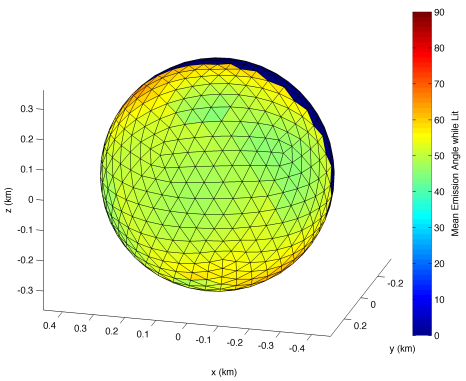

(c) Ping-Pong Orbit

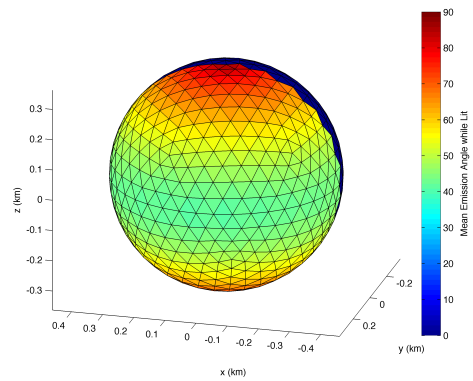

(d) Ecliptic Orbit

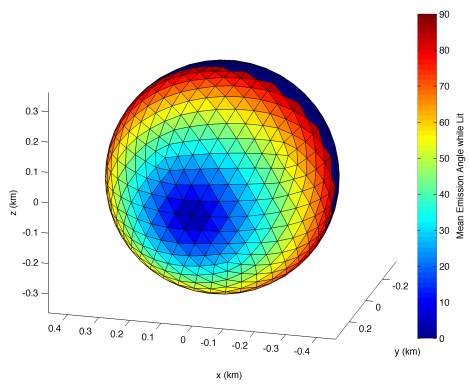

(e) Hover Orbit

Figure 10. Mean emisison angle while lit for example trajectories

orbits near the terminator). Both the QTO and ping-pong orbits possess higher standard deviation of the phase angle and relatively low standard deviation of the mean emission angle – both positive qualities. It is also important to note that the QTO is stable and requires no deterministic maneuvers while the ping-pong trajectory is clearly non-ballistic and requires maneuvers approximately every 10 days.

CONCLUDING REMARKS

This investigation is intended to provide a preliminary basis for comparison of different orbit approaches as they relate to carrying out a remote sensing campaign at a small primitive body. The importance of varied viewing geometry is emphasized primarily in terms of incidence and emission angle, though other metrics such as azimuth angle, spacecraft range, and surface coverage percentage are certainly relevant as well. To simplify and generalize the analysis, a spherical polyhedral body is used throughout this investigation, though the results should, in general, be applicable to a variety of trajectory and primitive body classes.

The achievable emission-incidence space is explored for five common types of mapping orbits. It is demonstrated that terminator orbits offer favorable coverage near the plane of the orbit, however, their achievable viewing geometries are quite limited because the phase angle of these orbits is always greater than 90 degrees. Assuming a primitive body pole that is parallel to ecliptic north (the P2 orientation) ecliptic orbits provide significantly better viewing opportunities than the terminator orbits at low to mid latitudes but significantly worse coverage near the polar regions. In this analysis, quasi-terminator orbits are shown to exhibit excellent incidence-emission coverage. A portion of incidence-emission space is not covered by quasi-terminators orbits due to the phase angle constraint, however, this constraint angle is typically much lower for quasi-terminator trajectories than for terminators. Both terminator and quasi-terminator trajectories have the significant operational advantage of generally being dynamically stable and requiring potentially less frequent stationkeeping. Hover orbits require regular orbit maintenance and are well-suited for obtaining a preliminary, narrow swath of viewing geometries, but are probably not well-suited for long-term, detailed surface mapping campaigns. Ping-pong trajectories are, in general, arbitrary so they have the potential for yielding unparalleled observation quality at the expense of propellant, maneuver frequency, and operational complexity.

The case study in this paper presents several useful metrics that are employed to quantitatively assess the relative quality of candidate mapping orbits for a spherical, phase-locked primitive body. Mean quantities and the standard deviation of mean quantities are leveraged to interpret the local and global variety of observation geometries achieved by a given trajectory. The orbital period and maneuver frequency offer insight into an orbit's operational complexity. Additional parameters for quantifying a trajectory's remote sensing capability certainly exist as well. As in the incidence-emission analysis, quasi-terminator and ping-pong orbits are again shown to exhibit the most favorable characteristics for surface mapping. While this analysis is largely preliminary, it is intended to make characterizing candidate mapping orbits more straightforward and to enable mission designers to make more informed decisions during preliminary mission design activities.

ACKNOWLEDGMENT

The work described in this paper was carried out at the Jet Propulsion Laboratory, California Institute of Technology, under a contract with the National Aeronautics and Space Administration.

REFERENCES

[1] D. Scheeres, "Orbit Mechanics about Small Asteroids," *AAS/AIAA Spaceflight Mechanics Meeting*, No. AAS 09-220, Savannah, Georgia, February 2009.

[2] G. Lantoine, S. Broschart, and D. Grebow, "Design of Quasi-terminator Orbits Near Primitive Bodies," *AAS/AIAA Astrodynamics Specialist Conference*, No. AAS 13-815, Hilton Head, South Carolina, August 2013.

[3] M. Wallace, S. Broschart, E. Bonifiglio, S. Bhaskharan, and A. Cangahuala, "Trajectory Design Considerations for Small-body Touch-and-go," *AAS/AIAA Space Flight Mechanics Meeting*, No. AAS 11-146, New Orleans, Louisiana, February 2011.

[4] H. Dankowicz, "Some Special Orbits in the Two-body Problem with Radiation Pressure," *Celestial Mechanics and Dynamical Astronomy*, Vol. 58, 1994, pp. 353–370.

[5] D. J. Scheeres, "Satellite Dynamics about Asteroids," *Advances in the Astronautical Sciences*, Vol. 87, 1994, pp. 275–292. AAS Paper 94-112.

[6] D. J. Scheeres, "Satellite Dynamics about Small Bodies: Averaged Solar Radiation Pressure Effects," *Journal of the Astronautical Sciences*, Vol. 47, No. 1, 1999, pp. 25–46.

[7] D. J. Scheeres, "Orbit Mechanics About Asteroids and Comets," *Journal of Guidance, Control and Dynamics*, Vol. 35, No. 3, 2012, pp. 987–997.

[8] S. B. Broschart and B. F. Villac, "Identification of Non-chaotic Terminator Orbits near 6489 Golevka," *Advances in the Astronautical Sciences*, Vol. 134, 2009, pp. 861–880. AAS Paper 09-156.

[9] B. S. D.J. Scheeres and A. Rosengren, "Design, Dynamics, and Stability of the OSIRIS-REx Sun-Terminator Orbits," *Advances in the Astronautical Sciences*, Vol. 148, 2013, pp. 3263–3282. AAS Paper 13-411.

[10] F. Mignard, "Radiation Pressure and Dust Particle Dynamics," *Icarus*, Vol. 49, 1982, pp. 347–366.

[11] D. Yárnoz, J.-P. Cuartielles, and C. McInnes, "Alternating Orbiter Strategy for Asteroid Exploration," *Journal of Guidance, Control, and Dynamics*, 2014, 10.2514/1.G000562.

[12] A. Krivov, L. Sokolov, and V. Dikarev, "Dynamics of Mars-orbiting Dust: Effects of Light Pressure and Planetary Oblateness," *Celestial Mechanics and Dynamical Astronomy*, Vol. 63, 1996, pp. 313–339.

[13] C. Colombo, C. Lucking, and C. McInnes, "Orbital Dynamics of High Area-to-mass Ratio Spacecraft with J2 and Solar Radiation Pressure for Novel Earth Observation and Communication Services," *Acta Astronautica*, Vol. 81, 2012, pp. 137–150.

[14] D. Lantukh, R. Russell, and S. Broschart, "Heliotropic orbits at oblate asteroids: balancing solar radiation pressure and J2 perturbations," *Celestial Mechanics and Dynamical Astronomy*, 2014, 10.1007/s10569-014-9596-x.

[15] M. Wallace and S. Broschart, "Circular-orbit Maintenance Strategies for Primitive Body Orbiters," *Advances in the Astronautical Sciences*, Vol. 150, 2013, pp. 1675–1687. AAS Paper 13-816.

[16] S. Broschart, G. Lantoine, and D. Grebow, "Quasi-terminator Orbits Near Primitive Bodies," *Celestial Mechanics and Dynamical Astronomy*, Vol. 120, 2014, pp. 195–215.

[17] M. Giancotti, S. Campagnola, Y. Tsuda, and J. Kawaguchi, "Families of periodic orbits in Hills problem with solar radiation pressure: application to Hayabusa 2," *Celestial Mechanics and Dynamical Astronomy*, Vol. 120, No. 3, 2014, pp. 269–286, 10.1007/s10569-014-9564-5.

[18] S. Sawai, D. J. Scheeres, and S. B. Broschart, "Control of Hovering Spacecraft using Altimetry," *Journal of Guidance, Control and Dynamics*, Vol. 25, No. 4, 2002, pp. 786–795.

[19] R. Furfaro, "Hovering in Asteroid Dynamical Environments Using Higher-Order Sliding Control," *Journal of Guidance, Control and Dynamics*, 2014, 10.2514/1.G000631.

[20] T. Kominato, M. Matsuoka, M. Uo, T. Hashimoto, and J. Kawaguchi, "Optical Hybrid Navigation and Station Keeping around Itokawa," presented at the AIAA/AAS Astrodynamics Specialist Conference, Keystone, CO, August 21-24, 2006, AIAA 2006-6535, 2006.

[21] J. Kawaguchi, A. Fujiwara, and T. Uesugi, "HayabusaIts technology and science accomplishment summary and Hayabusa-2," *Acta Astronautica*, Vol. 62, No. 1011, 2008, pp. 639 – 647, http://dx.doi.org/10.1016/j.actaastro.2008.01.028.

[22] Y. Tsuda, M. Yoshikawa, M. Abe, H. Minamino, and S. Nakazawa, "System Design of the Hayabusa 2 - Asteroid Sample Return Mission to 1999 JU3," *Acta Astronautica*, Vol. 91, 2013, pp. 356 – 362.

[23] D. Wokes and J. Essert, "Development of Rosetta's Initial Stage Comet Rendezvous Guidance Systems," presented at the AIAA/AAS Astrodynamics Specialist Conference, August 13-16, 2012, Minneapolis, Minnesota, 2012.

[24] W. V. Boynton, D. S. Lauretta, E. Beshore, O. Barnouin, E. B. Bierhaus, R. Binzel, P. R. Christensen, M. Daly, J. Grindlay, V. Hamilton, A. R. Hildebrand, G. Mehall, D. Reuter, B. Rizk, A. Simon-Miller, and P. S. Smith, "The OSIRIS-REx mission to RQ36: nature of the remote sensing observations," presentation slides from the European Planetary Science Congress 2012, 23 28 September 2012, Madrid, Spain, 2012.